Electronic Supplementary Information (ESI)
for the paper:

Modulation of self-assembly and magnetism of Cu(II) grids in solution

A. Electron paramagnetic resonance (EPR)

Technical.

The continuous wave EPR spectra were recorded at X-band (*ca.* 9~10 GHz) with a spectrometer (ESP-300-E, Bruker Spectrospin) equipped with a continuous He-flow cryostat (ESR 900, Oxford). Nutation pulsed EPR experiments were performed at X-band using a spectrometer (ELEXSYS 580, BRUKER Spectrospin) equipped with a continuous He-flow cryostat (CF 935, Oxford). Solutions were prepared according to the following procedures.

The complexes $[Cu_2\mathbf{1a}_2]^{4+}$, $[Cu_4\mathbf{1a}_4]^{8+}$ and $[Cu_4\mathbf{1b}_4]^{8+}$ have been prepared directly by mixing the stoichiometric amount of ligand and metal salt in CH_3CN, as described in the main text. All reported EPR data are given for this preparation.

The spin nutation data and EPR spectrum reported in the main text for the triazine-based grid $[Cu_4\mathbf{1b}_4]^{8+}$ are given for a solution prepared by dissolving solid $[Cu_4\mathbf{1b}_4]^{8+}$ within a 1:1:1 $CHCl_3/CH_3CN/CH_3OH$ mixture. This composition produced a good glassy matrix in the frozen state. Other sample preparations reported in this Supp. Inf. are given within figure captions.

All solutions were degassed by bubbling Ar directly in the EPR tube prior to measurements. Such a dilution allows isolating the entities so as focussing on the intramolecular magnetic exchange couplings. Temperature was measured with a thermocouple (AuFe/Chromel) located within the sample solution. Much care was devoted to the effects of microwave power saturation.
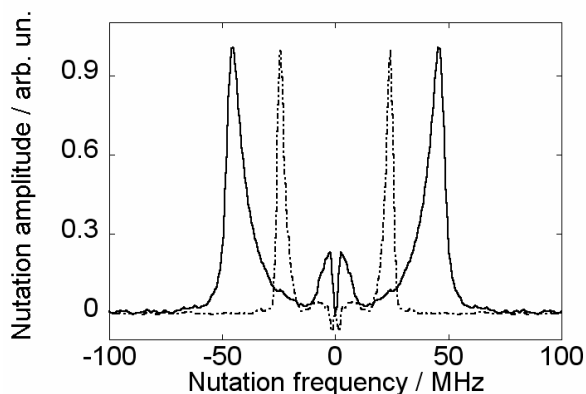
B. ***Spin nutation.***

In the described experimental conditions $\nu_{S=1/2}$ ~23 MHz (established by measurements with nitroxide free radicals).

The nutation frequencies are given by the following expression:[1]

$$\nu_{\mathrm{nut}} = \sqrt{S(S+1) - m_S(m_S+1)} \cdot \nu_{S=1/2}$$

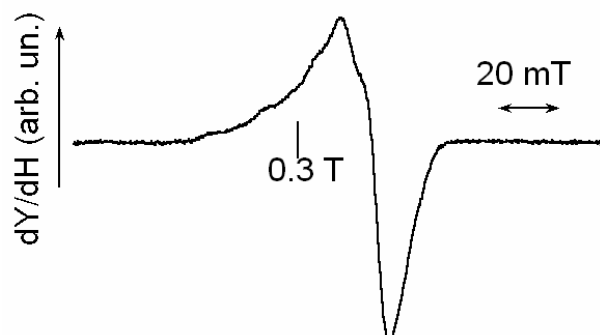This relation predicts $\nu_{S=2}=2\nu_{S=1/2}$ for $m_S=\pm1 \leftrightarrow m_S=\pm2$ transitions.

Figure S1. Nutation spectra of grids in frozen 1:1:1 $CHCl_3/CH_3CN/CH_3OH$ solution of $[Cu_4\mathbf{1a}_4]^{8+}$ (dash-dotted line) and $[Cu_4\mathbf{1b}_4]^{8+}$ (continuous line) at 6 K.
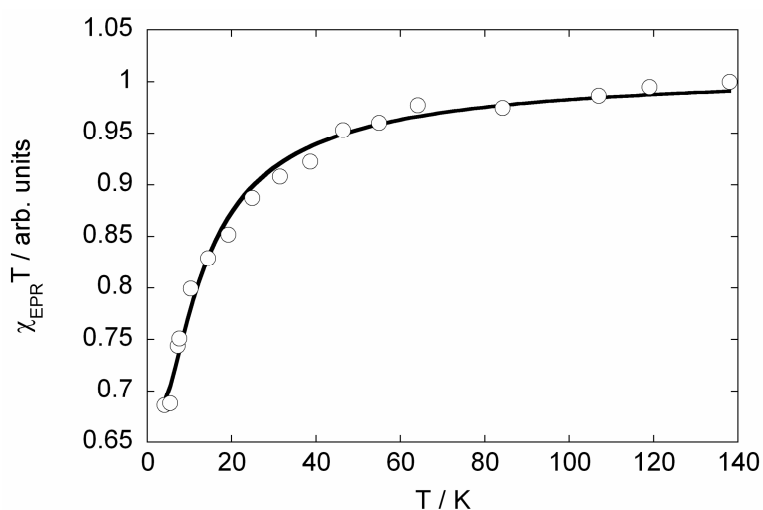
[1] S. Stoll, G. Jeschke, M. Willer, and A. Schweiger *J. Magn. Res.*, 1998, **130**, 86-96.

C. *EPR spectra and spin susceptibility.*
C.1. *Complexes of pyrimidine-based ligand 1a.*

Figure S2. X-band EPR spectrum recorded at 21 K for the frozen solution of the stick $[Cu_2\mathbf{1a}]^{4+}$, which EPR spectrum is given at 4 K in the main text.

Figure S3. Temperature dependence of the χT product obtained from the integrated EPR susceptibility of the pyrimidine based grid, compound $[Cu_4\mathbf{1a}_4]^{8+}$ in frozen 10^{-3} M/CH$_3$CN solution. The continuous line represents the fit (fit 1 in Table S1) corresponding to a [2x2] grid with a unique intra-grid antiferromagnetic exchange interaction ($J/k_B \cong$ -18 K) yielding an S=0 ground state and a Curie law for isolated S=1/2 spins.

According to the equilibriums of grid dissociation (See Figure S5) observed through visible and mass spectrometry, the S=1/2 contribution may be due to grid corners $[Cu\mathbf{1a}_2]^{2+}$ and/or grid quarters $[Cu\mathbf{1a}]^{2+}$ and/or to copper salt. Alternate fits give reasonable agreement with the experimental data. Those correspond to:

    i)   a mixture of 4-spin species (square grid $[Cu_4\mathbf{1a}_4]^{8+}$), 2-spin species (half-grid $[Cu_2\mathbf{1a}_2]^{2+}$), and 1-spin species (grid corner $[Cu\mathbf{1a}_2]^{2+}$, grid quarter $[Cu\mathbf{1a}_2]^{2+}$ and/or Cu^{2+} salt) (fit 2 in Table S1);

    ii)   A mixture of a 2-spin species (half-grid $[Cu_2\mathbf{1a}_2]^{2+}$) with 1-spin species (grid corner $[Cu\mathbf{1a}_2]^{2+}$, grid quarter $[Cu\mathbf{1a}_2]^{2+}$ and/or Cu^{2+} salt) (fit 3 in Table S1)

Two-spin stick-like species $[Cu_2\mathbf{1a}]^{4+}$ were not considered for the fit given that their formation requires a Cu:**1a** molar ratio equal to 2:1

Theoretical expressions used for the fits are as follows:

2

- 2-spin system (Bleaney-Bowers law): $\chi_2\,T = 2\,C f_2(J,T)$ with $f_2(J,T) = \dfrac{3}{3 + \exp(J_2 / k_B T)}$

- 4-spin system: $\chi_4\,T = C f_4(J,T)$ with $f_4(J,T) = \dfrac{6\,\exp(J/k_B T) + 12\,\exp(2J/k_B T) + 30\,\exp(3J/k_B T)}{1 + 3\,\exp(J/k_B T) + 7\,\exp(2J/k_B T) + 5\,\exp(3J/k_B T)}$

The Curie factor, $C = \dfrac{N g^2 \mu_B{}^2}{3 k_B}$ (0.5 emu.K.Mol^{-1} in absolute units for g=2.00) is common to all Curie constants in mixtures.

Therefore, fits are given by:

Fit 1: $\chi_{exp}\,T = C\left[x_4\,f_4(J,T) + 0.75(1 - x_4) \right]$

Fit 2: $\chi_{exp}\,T = C\left[x_4\,f_4(J,T) + 2 x_2\,f_2(J,T) + 0.75(1 - x_4 - x_2) \right]$

Fit 3: $\chi_{exp}\,T = C\left[2 x_2\,f_2(J,T) + 0.75(1 - x_2) \right]$

In these expressions, x_i is the fraction of i-spin systems (i=1,2,4), i.e. x_1 represents the fraction of S=1/2 isolated Cu^{2+} spin, according to the normalisation condition: $\sum_i x_i = 1$.

Table S1. Fit parameters to the expressions given as fit 1, fit 2, and fit 3. R^2 is the residual mean square; the fits concern compound [Cu$_4$**1a**$_4$]$^{8+}$ in frozen 10^{-3} M/CH$_3$CN solution.

	x_2 (%)	J_2/k_B (K)	x_4 (%)	J_4/k_B (K)	x_1 (%)	C (arb. un.)	R^2
Fit 1			10.8±0.5	-17.9±1.5	89.2±0.5	1.02±0.01	0.98967
Fit 2	5.4±1.9	-77.0±22.5	9.7±0.8	-11.9±2.5	84.9±2.7	1.02±0.02	0.99547
Fit 3	9.9±0.5	-25.7±2.3			90.1±0.5	1.03±0.01	0.98086

C.2. *Grid of triazine-based ligand 1b.*
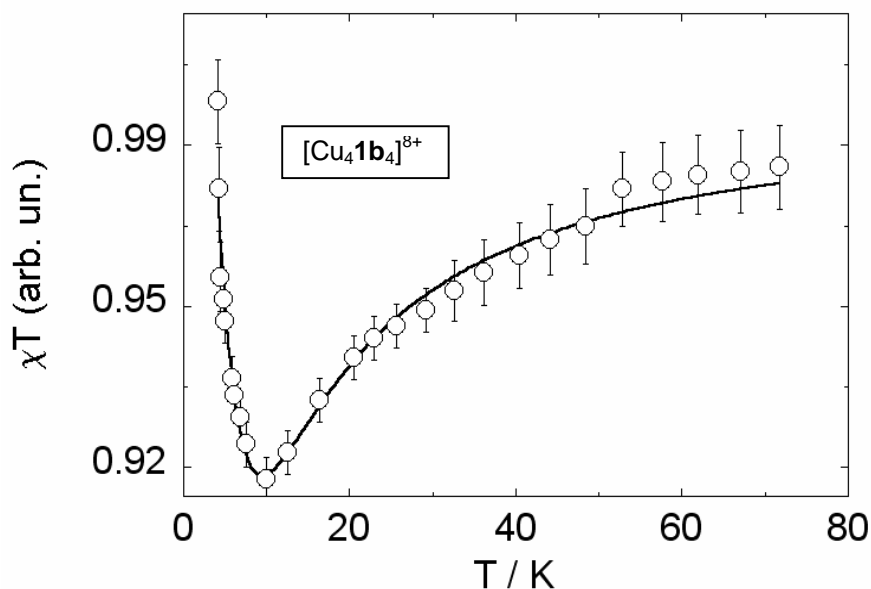
Figure S4. Temperature dependence of the integrated EPR absorption (EPR susceptibility) for complex [Cu$_4$**1b**$_4$]$^{8+}$ in frozen solution prepared by dissolving a polycrystalline powder of the grid within a 1:1:1 CHCl$_3$/CH$_3$CN/CH$_3$OH mixture (same sample than the one studied through spin nutation experiments). Continuous line holds for the theoretical fit for a mixture of two square grids in similar proportion with $(J_F, J_{AF})/k_B$=(+8K,-16K).

D. Crystallographic data

Crystals were growth by diffusion of a non-solvent (Et_2O for $[Cu_2\mathbf{1a}]^{4+}$ and $[Cu_4\mathbf{1a_4}]^{8+}$, $CHCl_3$ for $[Cu_4\mathbf{1b_4}]^{8+}$) into acetonitrile solutions of the complexes. The crystals were placed in oil, and a single crystal was selected, mounted on a glass fibre and placed in a low-temperature N_2 stream.

X-Ray diffraction data collection was carried out on a Nonius Kappa-CCD diffractometer[2] equipped with an Oxford Cryosystem liquid N_2 device, using graphite-monochromated Mo-Kα radiation (λ = 0.71073 Å). The crystal-detector distance was 36mm. The cell parameters were determined from reflections taken from one set of 10 frames (1.0° steps in phi angle), each at 20s exposure. The structure was solved by Direct methods using the programme SHELXS-97[3]. The refinement and all further calculations were carried out using SHELXL-97[4]. The H-atoms were included in calculated positions and treated as riding atoms using SHELXL default parameters. The non-H atoms were refined anisotropically, using weighted full-matrix least-squares on F2, except in the structure of compound $[Cu_4\mathbf{1a_4}]^{8+}$ where 3 molecules of acetonitrile solvent are in special position and refined isotropically. The hydrogen atoms of these 3 acetonitrile molecules are not located but are included in the formula. The SQUEEZE instruction in PLATON[4] has been applied to the data and the "squeezed" residual density corresponds to half a molecule of $CF_3SO_3^-$ plus 2 CH_3CN, too disordered to be modelled (very unstable crystal).

For compound $[Cu_2\mathbf{1a}]^{4+}$, a semi-empirical absorption correction was applied using the MULscanABS routine in PLATON; transmission factors: T_{min}/T_{max} = 0.658/0.928.

For compound $[Cu_4\mathbf{1b_4}]^{8+}$, it was not possible to locate the hydrogen of the molecule of water. It was decided to impose 50% occupancy for the molecules water because of the high value of the thermal agitation parameter of these molecules.

CCDC 753682 ($[Cu_4\mathbf{1b_4}]^{8+}$), 753683 ($[Cu_2\mathbf{1a}]^{4+}$) and 778853 ($[Cu_4\mathbf{1a_4}]^{8+}$) contain the supplementary crystallographic data for this paper. These data can be obtained free of charge from the Cambridge Crystallographic Data Centre via www.ccdc.cam.ac.uk/data_request/cif.

---

[2] Kappa CCD Operation Manual, Nonius B. V., Ed.; Delft: The Netherlands, 1997.

[3] G. M. Sheldrick, (1990) "SHELXS-97 Program for Crystal Structure Determination", *Acta Crystallogr.*, **A46**, 467-473.

[4] G. M. Sheldrick, (1997) "SHELXL-97", Universität Göttingen, Göttingen, Germany.

Table S2. Crystal data

Compound	$[Cu_2 1a]^{4+}$	$[Cu_4 1a_4]^{8+}$	$[Cu_4 1b_4]^{8+}$
Chemical formula	$C_{26}H_{26}Cu_2F_{12}N_{10}O_{13}S_4$	$C_{90}H_{87}Cu_4F_{24}N_{37}O_{24}$	$C_{210}H_{186}Cl_{18}Cu_8F_{48}N_{74}O_{51}S_{16}$
$M/g\,mol^{-1}$	1169.89	3037.61	7133.71
Crystal system	Triclinic	Orthorhombic	Monoclinic
Space group	P-1	Pnma	P21/n
$a/Å$	10.3216(3)	23.0185(4)	18.406(2)
$b/Å$	11.1123(3)	20.8028(3)	41.162(5)
$c/Å$	19.8965(5)	28.2909(6)	20.075(2)
$\alpha/°$	87.112(2)	90	90
$\beta/°$	82.405(2)	90	107.58(2)
$\gamma/°$	69.908(1)	90	90
$V/Å^3$	2124.35(10)	13547.1(4)	14499(3)
Z	2	4	2
$D_{calcd.}/g\,cm^{-3}$	1.829	1.489	1.633
$\lambda/Å$	0.71073 (Mo-Kα)	0.71073 (Mo-Kα)	0.71073 (Mo-Kα)
μ/mm^{-1}	1.322	0.851	0.969
F(000)	1172	6152	7184
T/K	173	173	173
R	0.0511	0.1047	0.0944
wR_2	0.1640	0.3277	0.3015
GOF	1.061	1.035	1.028
$\Delta\rho_{min}/e\,Å^{-3}$	-0.98	-1.37	-1.03
$\Delta\rho_{max}/e\,Å^{-3}$	1.32	1.51	1.56
CCDC #	753683	778853	753682

E. Table S3. Mass spectrometry results

Complex	Cationic fragment observed	Formula	m/z Calcd. (100%)	m/z Obs.
$[Cu_2\mathbf{1a}]^{4+}$	$[Cu_2\mathbf{1a}](OTf)_3^+$	$C_{21}H_{18}Cu_2F_9N_8O_9S_3$	920.878	920.881
	$[Cu_2\mathbf{1a}](OTf)_2^{2+}$	$C_{20}H_{18}Cu_2F_6N_8O_6S_2$	385.963	385.964
	$[Cu\mathbf{1a}](OTf)^+$	$C_{19}H_{18}CuF_3N_8O_3S$	558.047	558.047
$[Cu_4\mathbf{1a}_4]^{8+}$	$[Cu_4\mathbf{1a}_4](OTf)_6^{2+}$	$C_{78}H_{72}Cu_4F_{18}N_{32}O_{18}S_6$	1267.045	1267.051
	$[Cu_2\mathbf{1a}_2](OTf)_3^+$	$C_{38}H_{36}Cu_2F_6N_{16}O_6S_2$	1267.044	1267.051
	$[Cu\mathbf{1a}_2](OTf)^+$	$C_{37}H_{36}CuF_3N_{16}O_3S$	904.212	904.223
	$[Cu\mathbf{1a}](OTf)^+$	$C_{19}H_{18}CuF_3N_8O_3S$	558.047	558.051
$[Cu_4\mathbf{1b}_4]^{8+}$	$[Cu_4\mathbf{1b}_4](OTf)_6^{2+}$	$C_{98}H_{84}Cu_4F_{18}N_{36}O_{18}S_6$	1421.099	1421.131
	$[Cu_4\mathbf{1b}_4](OTf)_5^{3+}$	$C_{97}H_{84}Cu_4F_{15}N_{36}O_{15}S_5$	897.748	897.774
	$[Cu_4\mathbf{1b}_4](OTf)_4^{4+}$	$C_{96}H_{84}Cu_4F_{12}N_{36}O_{12}S_4$	636.073	636.107
	$[Cu\mathbf{1b}](OTf)^+$	$C_{24}H_{21}CuF_3N_9O_3S$	635.073	635.098

F. Table S4. Visible spectroscopy

Complex	Total ligand concentration (M)	Theoretical concentration of complexes (M)	λ_{max} (nm)	ε (M^{-1}cm^{-1})* (uncertainty ± 5%)
$[Cu_2\mathbf{1a}]^{4+}$	10^{-2}	10^{-2}	656	203
	$8\cdot10^{-3}$	$8\cdot10^{-3}$	656	198
	$6\cdot10^{-3}$	$6\cdot10^{-3}$	654	198
	$4\cdot10^{-3}$	$4\cdot10^{-3}$	654	201
	$2\cdot10^{-3}$	$2\cdot10^{-3}$	653	199
	10^{-3}	10^{-3}	654	204
$[Cu_4\mathbf{1a}_4]^{8+}$	10^{-2}	$0.25\cdot10^{-2}$	694	324
	$8\cdot10^{-3}$	$2\cdot10^{-3}$	693	325
	$6\cdot10^{-3}$	$1.5\cdot10^{-3}$	690 (blue shift)	321
	$4\cdot10^{-3}$	10^{-3}	683	332
	$2\cdot10^{-3}$	$0.5\cdot10^{-3}$	662	371
	10^{-3}	$0.25\cdot10^{-3}$	638	440
$[Cu_4\mathbf{1b}_4]^{8+}$	10^{-2}	$0.25\cdot10^{-2}$	744	283
	$8\cdot10^{-3}$	$2\cdot10^{-3}$	743	288
	$6\cdot10^{-3}$	$1.5\cdot10^{-3}$	745	285
	$4\cdot10^{-3}$	10^{-3}	744	286
	$2\cdot10^{-3}$	$0.5\cdot10^{-3}$	744	289
	10^{-3}	$0.25\cdot10^{-3}$	745	288

* average values